Published OnlineFirst April 27, 2018; DOI: 10.1158/1078-0432.CCR-17-2602

Translational Cancer Mechanisms and Therapy

Clinical Cancer Research

Insulin-Like Growth Factor 2 mRNA-Binding Protein 3 is a Novel Post-Transcriptional Regulator of Ewing Sarcoma Malignancy

Caterina Mancarella[1], Michela Pasello[1], Selena Ventura[1], Andrea Grilli[1], Linda Calzolari[1], Lisa Toracchio[1], Pier-Luigi Lollini[2], Davide Maria Donati[3], Piero Picci[4], Stefano Ferrari[5], and Katia Scotlandi[1]

Abstract

Purpose: Large-scale sequencing studies have indicated that besides genomic alterations, the posttranscriptional regulation of gene expression or epigenetic mechanisms largely influences the clinical behavior of Ewing sarcoma. We investigated the significance of the RNA-binding protein IGF2BP3 in the regulation of Ewing sarcoma aggressiveness.

Experimental Design: Explorative study was performed in 14 patients with localized Ewing sarcoma using RNA sequencing. Next, 128 patients with localized Ewing sarcoma were divided into two cohorts. In the training set, 29 Ewing sarcoma samples were analyzed using Affymetrix GeneChip arrays. In the validation set, 99 Ewing sarcoma samples were examined using qRT-PCR. Patient-derived cell lines and experimental models were used for functional studies.

Results: Univariate and multivariate analyses indicated *IGF2BP3* as a potent indicator of poor prognosis. Furthermore, *ABCF1* mRNA was identified as a novel partner of IGF2BP3. Functional studies indicated IGF2BP3 as an oncogenic driver and *ABCF1* mRNA as a sponge that by binding IGF2BP3, partly repressed its functions. The combined evaluation of *IGF2BP3* and *ABCF1* could identify different patient outcomes—high *IGF2BP3* and low *ABCF1* levels indicated poor survival (25%), whereas low *IGF2BP3* and high *ABCF1* levels indicated favorable survival (85.5%). The bromodomain and extraterminal domain inhibitor (BETi) JQ1 decreased IGF2BP3 expression, modified the expression of its validated targets and inhibited the capability of Ewing sarcoma cells to grow under anchorage-independent conditions.

Conclusions: The combined assessment of *IGF2BP3* and *ABCF1* predicts recurrence in Ewing sarcoma patients. Thus, for patients with high expression of IGF2BP3 and poor probability of survival, the use of BETis should be clinically evaluated. *Clin Cancer Res; 24(15); 3704–16. ©2018 AACR.*

Introduction

Pediatric cancers have a generally quiet genome. However, epigenetic changes are common and may constitute an important class of drivers for these diseases. Ewing sarcoma, a rare disease with unmet clinical needs and relevant social impact on pediatric and young adult population, is no exception. Large-scale genomic sequencing studies have demonstrated that Ewing sarcoma has one of the lowest mutation rates among all cancers (0.15 mutations/Mb), thereby resulting in a paucity of pharmacologically actionable mutations (1–3). Thus, Ewing sarcoma treatment has not benefited from the most recent genetic technologies, and it is still entrapped with the use of dose-dense chemotherapy in combination with surgery and/or radiation. Ewing sarcoma prognosis continues to be poor for metastatic and recurrent patients, with much scope for improvement (4), while Ewing sarcoma survivors report harsh performance limitations with restriction of routine activities as a consequence of treatment morbidities that severely impact their quality of life (5). To maximize the efficacy of standard treatments while limiting unnecessary toxicity, it is thus important to identify indicators of patient survival for the design of risk-based therapies. Recent genome-scale DNA methylation sequencing for a large cohort of Ewing sarcoma tumors (6) indicated a substantial epigenetic heterogeneity within tumors that likely reflects the diverse clinical presentation and progression of Ewing sarcoma. However, in contrast with many other cancers, DNA methylation differences among Ewing sarcoma tumors did not uncover discrete subtypes but instead demarcated a continuous spectrum defined by mesenchymal versus stem cell signatures, which might reflect the differentiation state of the cell-of-origin and/or the strength of the regulatory signature imposed by EWS-FLI, the oncogenic driver of Ewing sarcoma. EWS-FLI functions primarily as a transcription factor that in addition to regulating the expression of specific targets

[1]CRS Development of Biomolecular Therapies, Experimental Oncology Laboratory, Orthopedic Rizzoli Institute, Bologna, Italy. [2]Department of Experimental, Diagnostic and Specialty Medicine, University of Bologna, Bologna, Italy. [3]Third Orthopedic Clinic and Traumatology, Orthopedic Rizzoli Institute, Bologna, Italy. [4]Experimental Oncology Laboratory, Orthopedic Rizzoli Institute, Bologna, Italy. [5]Musculoskeletal Tumors Chemotherapy Section, Orthopedic Rizzoli Institute, Bologna, Italy.

Note: Supplementary data for this article are available at Clinical Cancer Research Online (http://clincancerres.aacrjournals.org/).

Corresponding Authors: Katia Scotlandi, CRS Development of Biomolecular Therapies, Experimental Oncology Laboratory, Orthopedic Rizzoli Institute, Via di Barbiano 1/10, Bologna 40136, Italy. Phone: 39 051 6366760; Fax: 39 051 6366763; E-mail: katia.scotlandi@ior.it; and Caterina Mancarella, Phone: 39 051 6366937; E-mail: caterina.mancarella@ior.it

doi: 10.1158/1078-0432.CCR-17-2602

Published OnlineFirst April 27, 2018; DOI: 10.1158/1078-0432.CCR-17-2602

Translational Relevance

In this article, for the first time, we highlight the value of the RNA-binding protein IGF2BP3 in the regulation of Ewing sarcoma aggressiveness. IGF2BP3 acts as an oncogene, and its functions are counteracted by the sponging activities of the *ABCF1* mRNA, a novel target of IGF2BP3. In this study, we provided evidence of a direct interaction between these molecules and the steady-state regulation of *ABCF1* by IGF2BP3. We propose the use of a bromodomain and extraterminal domain inhibitor (BETi), which has marked antitumor activity, as a possible treatment strategy for patients with high expression of IGF2BP3 and low expression of ABCF1. These patients are prone to have poor prognoses, and BETi, by decreasing IGF2BP3 expression, may shift the balance toward lower disease aggressiveness and better outcomes.

interacts with multiple partners involved in transcriptional and splicing machineries (7). As a result, EWS-FLI orchestrates multiple oncogenic hits that lead to the transformation and disruption of normal developmental processes. Despite being a necessary condition, EWS-FLI is not sufficient to generate a fully transformed phenotype and requires adjuvant factors (3, 8). These data highlight the importance of investigating posttranscriptional mechanisms, including noncoding RNAs and RNA-binding proteins (RBPs), involved in gene expression regulation. Although noncoding RNAs have been found to be differentially expressed in Ewing sarcoma samples (9–11), and prognostic value has been established for some of them (12), the role of RBPs has been barely explored in Ewing sarcoma.

RBPs affect critical steps of posttranscriptional regulation, including mRNA maturation, splicing, translation, and stability (13). Taking advantage of two different throughput datasets generated in our laboratory by RNA sequencing (RNA-seq) and gene expression profiling in Ewing sarcoma patients who either responded or not to standard therapy, we investigated the implication of the expression of insulin-like growth factor 2 mRNA-binding proteins (IGF2BPs) in Ewing sarcoma progression and response to therapy (14). IGF2BPs are a conserved family of structurally and functionally related RBPs that bind mRNAs via 6 RNA-binding domains controlling cytoplasmic stability and translation of transcripts (reviewed in refs. 15, 16). Consisting of three paralogs (IGF2BP1, 2, and 3), these RBPs are oncofetal proteins with high expression during embryogenesis, low expression in adult tissues, and reexpression in malignancies. In epithelial cancers, IGF2BPs are emerging as promising outcome predictors and drug sensitivity regulators (17, 18), while in lymphatic tumors, IGF2BP3 upregulation represents a key mechanism operating in MLL-rearranged B-cell acute lymphoblastic leukemia (B-ALL; ref. 19). In this study, we identify the expression of *IGF2BP3*, but not of *IGF2BP1* or *2*, as a major indicator of adverse prognosis in Ewing sarcoma patients. We also discover *ABCF1* as a novel mRNA target of IGF2BP3 in Ewing sarcoma that counteracts the oncogenic potential of IGF2BP3 by preventing its association with some canonical oncogenic targets such as *MMP9*, *CD44*, and *ABCG2*. Contemporary assessment of *IGF2BP3* and *ABCF1* gene expression enabled the fine-tuned stratification of Ewing sarcoma patients based on outcomes. The selective bromodomain and extraterminal domain inhibitor (BETi) JQ1 reduced the levels of IGF2BP3 and its mRNA targets and may thus be considered for the treatment of high-risk patients.

Materials and Methods

Patient selection

Patients with localized Ewing sarcoma who were enrolled in prospective studies and treated at the Rizzoli Institute were included in the current analysis (20, 21). All patients had a diagnosis of Ewing sarcoma made on representative specimens from open or needle biopsies and based on histologic, cytologic, IHC features, as well as molecular presence of the chimeric product derived from Ewing sarcoma–specific chromosomal translocations (22, 23). Local treatment, performed after induction chemotherapy, consisted of radiotherapy, surgery, or surgery followed by radiotherapy. In patients locally treated with surgery, histologic response to chemotherapy was evaluated according to the method proposed by Picci and colleagues (24).

Explorative analysis was performed on 14 biopsies of patients with localized tumor with different outcomes analyzed by RNA-seq. A training set of 29 cases, previously profiled for gene expression (14), and a validation set of 99 cases comprised the study population. The patients' clinical characteristics are summarized in Supplementary Table S1. Clinical and follow-up data were updated to June 2014. The median follow-up of the population was 72 months (range 4–263 months). The rate of 5-year relapse-free survival (RFS) and overall survival (OS) was 60.9% and 70.3%, respectively.

The statistical power of samples included in the validation set was verified (index: 1), indicating adequate sample size (25). The ethical committee of the Rizzoli Institute approved the study (0041040/2015), and informed consent was obtained. The study was conducted in accordance with the Declaration of Helsinki ethical guidelines.

Sample processing for molecular analysis

Total RNA from snap-frozen tissue samples and/or cell lines was isolated using TRIzol Reagent (Invitrogen). RNA quality and quantity were assessed by NanoDrop analysis (NanoDrop ND1000, Thermo Fisher Scientific) and/or by electrophoresis. To check whether the extracted RNA was representative of Ewing sarcoma, tissue sections from the same snap-frozen tissue samples subjected to RNA extraction were morphologically analyzed with hematoxylin–eosin staining, and the slides were evaluated by a pathologist who certified the high-density cancer areas (>70%) before any processing as reported previously (9, 12). Tissues nonrepresentative of Ewing sarcoma were excluded. Details for quantitative real-time PCR (qRT-PCR) are in Supplementary Methods.

RNA-seq and bioinformatics analyses

Total RNA from snap-frozen tissue samples was extracted with TRIzol reagent. A total of 250–1,000 ng of total RNA was used for the synthesis of cDNA libraries with TruSeq RNA Sample Prep Kit v2 (Illumina) according to the manufacturer's recommendations and sequenced by synthesis using the 75-bp paired-end mode on HiScanSQ sequencer (Illumina). Raw reads were aligned using TopHat (version 2.1.0; ref. 26) to build version hg19 of the human genome from University of

Published OnlineFirst April 27, 2018; DOI: 10.1158/1078-0432.CCR-17-2602

California, Santa Cruz (Santa Cruz, CA). Counts for UCSC-annotated genes were calculated from the aligned reads using HTSeq (version 0.6.0; ref. 27). Normalization and differential analysis were carried out using edgeR package (version 2.12.0; ref. 28) and R (version 3.2.2). Raw counts were normalized according to library size to obtain counts per million (cpm). Only genes with a cpm greater than 1 in at least 3 samples were retained for differential analysis. Edger in R was used to identify gene expression modulation of coding genes. From the total list of 25,369 annotated genes, after filtering out genes with no expression (no more than 1 cpm in 3 samples), we obtained a total of 16,531 genes. A total of 595 genes were differentially expressed, 97 of which were noncoding genes (excluding genes with "protein_coding" class according to Ensembl hg19 annotation). Genes were tested for differential expression using the empirical Bayes moderation *t* statistics of the *limma* package (v. 3.30) and considered significant if the *P* value was $\leq$ 0.05 and the absolute fold change (F.C.) was $\geq$ 1.5.

Preclinical studies

Functional studies were performed on 9 patient-derived Ewing sarcoma cell lines authenticated by DNA fingerprinting (last control December 2017) and found to be mycoplasma-free by MycoAlert mycoplasma detection kit (Lonza; control every 3 months). A673 and TC-71 cells were stably silenced for IGF2BP3 after transfection with pLKO.1 vector containing the *IGF2BP3*-specific short hairpin RNA (TRCN0000074673) and selected with puromycin (2 μg/mL, Sigma). Transient overexpression of IGF2BP3 was achieved by transfecting LAP-35 cells with the pCDH vector containing *IGF2BP3* cDNA. The details are in Supplementary Methods.

In vivo studies

Six-week-old female athymic Crl:CD-1-nu/nu Br mice, hereafter referred to as "nude" mice (Charles River), were used. A total of 2×10^6 viable cells were injected in lateral tail veins of mice. The care of mice and experimental protocols were reviewed and approved by the Institutional Animal Care and Use Committee ("Comitato per il Benessere Animale") of the University of Bologna and by the Italian Ministry of Health letter 208/2017-PR. The details are in Supplementary Methods.

Statistical analysis

Association between *IGF2BP3* expression and RFS or OS was estimated by Cox proportional hazards regression analysis. RFS and OS were plotted using the Kaplan–Meier method, while the log-rank test was used to calculate univariate statistical significance of observed differences. RFS was calculated as the time from diagnosis to occurrence of adverse events defined as recurrence or metastases at any site. OS was defined as the time from diagnosis to cancer-related death. Survivors or patients who were lost to follow-up were censored at the last contact date. All factors significantly associated with RFS and/or OS in univariate analysis were entered into a Cox proportional hazards model using stepwise selection multivariate analysis. Values of 95% confidence interval (CI) of hazard ratios (HRs) are provided (29). Differences among means were analyzed using Student *t* tests or the nonparametric Mann–Whitney rank-sum test when the data were not normally distributed. Experimental data including more than two groups were analyzed using one-way ANOVA. Fisher exact test was used to determine association between *IGF2BP3* expression and metastases incidence in mice. Spearman rank or Pearson tests were used to evaluate correlations. To define drug–drug interactions, the combination index (CI) was calculated with an isobologram equation using CalcuSyn software (Biosoft) to identify synergistic (CI < 0.9), additive ($0.9 \leq CI \geq 1.1$), or antagonistic (CI > 1.1) effects according to Chou and colleagues (30). All *P* values were two-sided. $P < 0.05$ was considered statistically significant. Statistical analyses were performed with SPSS software, version 22.0. Statistical power was calculated by PS Power and Sample Size Calculations, version 3.0.

Results

High expression of *IGF2BP3* in primary tumors predicts poor prognosis of Ewing sarcoma patients

To search for RBPs whose expression is associated with differential prognosis, we performed explorative RNA-seq of 14 biopsy samples (Supplementary Table S1) from primary localized Ewing sarcoma and compared fusions, mutations, and gene expression profiles between patients who did not experience recurrence (defined as patients with no evidence of disease, NED) and patients who experienced tumor progression within 3 years from diagnosis (defined as patients experiencing a relapse, REL). According to previous studies, we found no translocation other than the canonical EWS/ETS, typical of Ewing sarcoma, and the mutations were limited to *TP53* and *STAG2*. Mutations in *TP53* were more frequent in patients with poor response to treatments (4/7 in poor responders and 0/7 in good responders), confirming the prognostic value of *TP53* in Ewing sarcoma (3, 31). Gene expression analysis identified 595 genes (299 upregulated and 296 downregulated) with significant changes in expression levels between NED and REL patients ($P < 0.05$; one-way ANOVA). Among the most upregulated genes, we identified the RBP *IGF2BP3* (Supplementary Tables S2 and S3). Of note, the speculation for a clinical role of *IGF2BP3* also stemmed from our prior study that identified *IGF2BP3* among 20 genes in a genetic signature classifying patients experiencing critical disease progression, with a 100% classification performance (14). Expression analysis of three members of the IGF2BP family by microarray in a training set with 29 primary tumors (ref. 14; Supplementary Table S1) confirmed that *IGF2BP3*, but not *IGF2BP1* or *2* (Supplementary Fig. S1A and S1B), is differentially expressed in REL patients versus NED patients and in living patients versus patients who died of disease ($P = 0.0455$; $P = 0.0016$, Mann–Whitney test, respectively; Fig. 1A). The relation between the high expression of *IGF2BP3* and adverse outcomes was confirmed in the validation set using qRT-PCR ($P = 0.0124$, Mann–Whitney test; Supplementary Tables S1 and S4; Table 1; Fig. 1B). *IGF2BP3* was generally overexpressed in tumor specimens compared with that in human-derived mesenchymal stem cells (hMSCs) used as controls (median = 4.16; range = −3.75–13.01 vs. hMSC196; Supplementary Fig. S1C).

Cox proportional hazard regression analysis demonstrated an association between *IGF2BP3* and RFS or OS in the training [HR = 1.82; 95% CI (1.20–2.77); $P = 0.004$ or HR = 2.49; 95% CI (1.54–4.03); $P < 0.0001$, respectively] and validation sets [HR = 2.19; 95% CI (1.06–4.54); $P = 0.034$ or HR = 3.49; 95% CI (1.58–7.72); $P = 0.002$, respectively]. Next, median and 75th percentile values were used to stratify patients as high- or low-expressing in

Published OnlineFirst April 27, 2018; DOI: 10.1158/1078-0432.CCR-17-2602

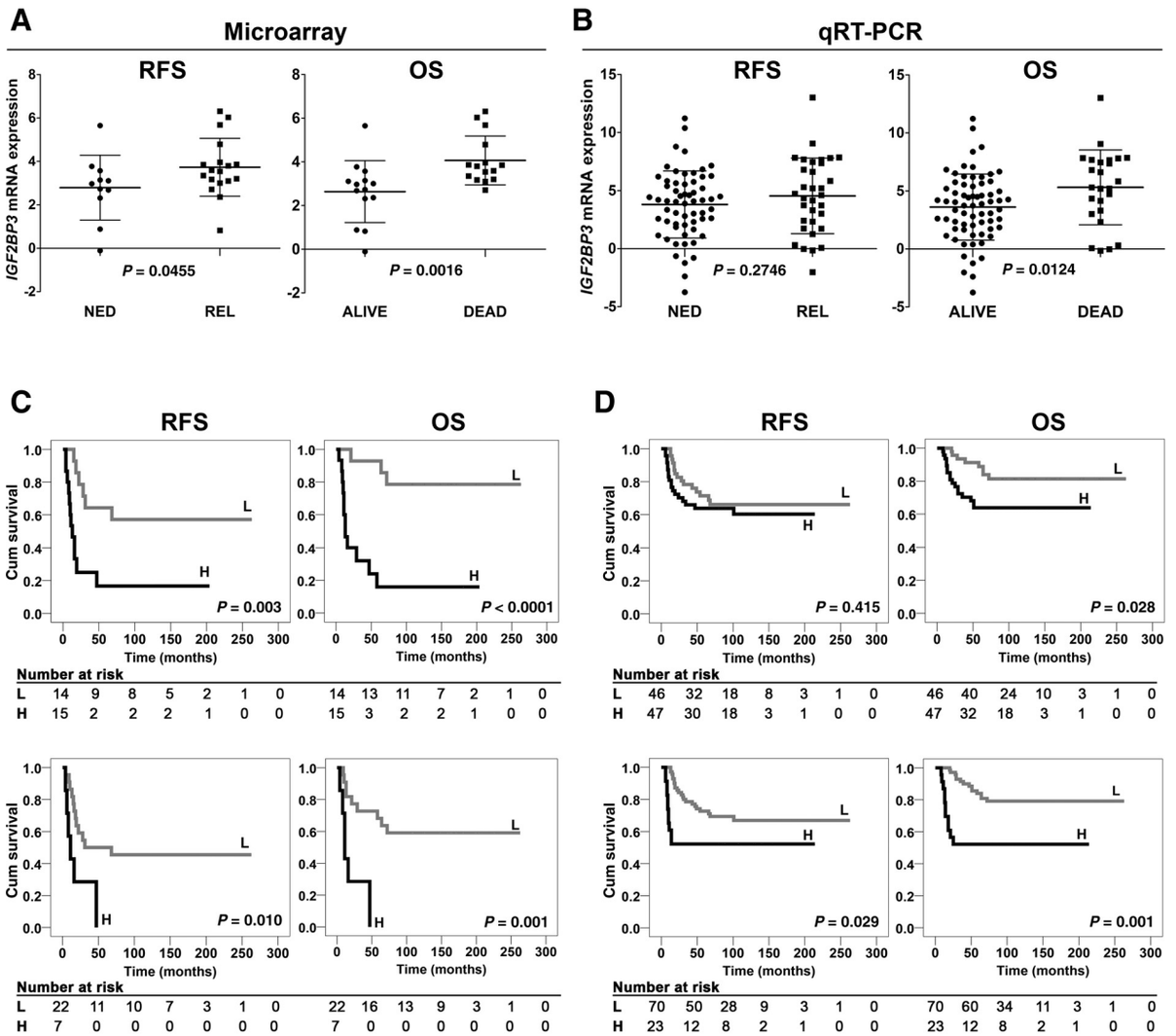

Figure 1.

Prognostic value of *IGF2BP3* in primary Ewing sarcoma patients. Scatter plot analysis of *IGF2BP3* expression in (**A**) 29 Ewing sarcoma cases analyzed by microarrays or in (**B**) 99 Ewing sarcoma cases evaluated by qRT-PCR. Differential expression between NED or REL and alive or dead patients was established by Mann–Whitney rank-sum test, and *P* values are displayed. Mean ± SD of relative mRNA expression ($2^{-\Delta\Delta C_t}$) reported as $\log_2$ is shown. Mean expression of two bone marrow-derived MSC (**A**) or hMSC196 (**B**) were used as calibrators. Prognostic impact of *IGF2BP3* expression according to Kaplan–Meier curves and log-rank test in 29 cases analyzed by microarrays (**C**) or in 99 cases evaluated by qRT-PCR (**D**). Samples with high (H) and low (L) expression were defined according to the median values (top panels) or the 75th percentile values (bottom). RFS and OS were evaluated. Time scale refers to months from diagnosis. The number of patients at risk in H and L samples are listed below each time interval.

the training and validation sets. The 75th percentile, which indicated very high expression of the molecule, better discriminated patients with different prognoses than did the median value, indicating that the levels of expression are critical for patient outcomes. Furthermore, Kaplan-Meier curves confirmed that the very high expression of *IGF2BP3* significantly affects either RFS or OS of Ewing sarcoma patients (Fig. 1C and D). Multivariate analysis was performed in the validation set for variables associated with RFS or OS identified by univariate analysis and confirmed high levels of *IGF2BP3* and poor response of tumors after neoadjuvant chemotherapy as independent risk factors of poor outcomes (Table 1).

IGF2BP3 increases anchorage-independent growth and migration in Ewing sarcoma cells

The expression of IGF2BP3 was investigated both at mRNA and protein levels in a panel of 9 Ewing sarcoma patient-derived cell lines compared with that in hMSCs (hMSC196). With the notable exception of two Ewing sarcoma cell lines (H-1474-P2 and H825), tumor cells expressed IGF2BP3 at higher levels than did normal cells (Fig. 2A). The expression of IGF2BP3 was not dependent on the expression of EWS-FLI, as demonstrated in A673 cells, in which inducible silencing of EWS-FLI did not modify the expression of IGF2BP3 (Supplementary Fig. S2). In the panel of Ewing sarcoma cell lines, a statistical correspondence

Published OnlineFirst April 27, 2018; DOI: 10.1158/1078-0432.CCR-17-2602

Table 1. RFS and OS log-rank and Cox proportional hazards regression multivariate tests in 99 Ewing sarcoma patients evaluated for *IGF2BP3* expression by qRT-PCR

		RFS			OS		
Characteristics	***n***	***P*-Univariate**	**HR (95% CI)**	***P*-Multivariate**	***P*-Univariate**	**HR (95% CI)**	***P*-Multivariate**
Gender		0.192			0.251		
Female	29						
Male	70						
Age		0.725			0.791		
$\leq$ 14 years	40						
> 14 years	59						
Location		0.06			0.253		
Extremity	77						
Central	7						
Pelvis	15						
LDH[a]		0.037		NS	0.008		NS
Normal	66						
High	25						
Surgery		0.165			0.037		NS
YES	90						
NO	9						
Local treatment		0.368			0.093		
RxT	9						
RxT + Surgery	20						
Surgery	70						
Response to chemotherapy[b]		0.008		0.01	0.008		0.01
Good	37		1			1	
Poor	53		1.74 (1.1–2.74)			2.11 (1.14–3.9)	
IGF2BP3[c]		0.029		0.05	0.001		0.005
Low	70		1			1	
High	23		2.14 (0.98–4.67)			3.49 (1.47–8.33)	

Abbreviations: LDH, lactate dehydrogenase; NS, not significant; OS, overall survival; RFS, relapse-free survival; RxT, radiotherapy.
[a]Data available for 91 cases.
[b]Data available for 90 cases.
[c]Data available for 93 cases divided as high and low expressers using 75th percentile.

was observed between mRNA and protein levels of IGF2BP3 ($r = 0.667$, $P = 0.05$, Spearman test). The protein expression of IGF2BP3 was directly correlated with the capability of Ewing sarcoma cells to form colonies under anchorage-independent conditions ($r = 0.767$, $P = 0.016$, Spearman test; Fig. 2B), one of the best *in vitro* parameters of malignancy (32). In contrast, no correlation was observed between IGF2BP3 levels and proliferation rate or sensitivity to drugs used in the therapy of Ewing sarcoma (not shown). This evidence was in line with the stronger capability of IGF2BP3 to predict OS rather than RFS, which reflects drug response more than general tumor aggressiveness. To confirm the role of IGF2BP3, A673 and TC-71 Ewing sarcoma cells, representative of those Ewing sarcoma cell lines with the highest IGF2BP3 expression and malignant features, were employed for loss-of-function studies. Cells depleted of IGF2BP3 (Fig. 2C; Supplementary Fig. S3A) displayed no variations in the sensitivity to vincristine (VCR) and doxorubicin (DXR) (Supplementary Fig. S3D and S3E) but showed few and small colonies in soft agar (Fig. 2D; Supplementary Fig. S3B), increased homotypic aggregation, and reduced cell migration (Fig. 2E; Supplementary Fig. S3C) and lower metastatic potential in nude mice (Supplementary Table S5). In addition, compared with those in control mice, the incidence of lymph node metastases was significantly decreased ($P = 0.034$, Fisher exact test), and lungs were less invaded (as shown by decreased lung weight) in mice injected with A673 IGF2BP3-silenced cells (Supplementary Table S5). Accordingly, the survival of mice injected with shIGF2BP3 #18 and #54 cells was significantly improved (Fig. 2F).

IGF2BP3 modulates the expression of *ABCF1*, a novel mRNA target, and *IGF2BP3-ABCF1* mRNA interaction identifies patients with different outcomes

IGF2BP3 contributes to cancer aggressiveness by regulating specific mRNAs (reviewed in ref. 16). Considering that validated IGF2BP3 targets, such as *MMP9*, a metalloproteinase involved in cell migration and invasion, *CD44*, a cell surface glycoprotein with a role in invadopodia formation, *ABCG2*, an ATP-binding cassette (ABC) transporter with a key role in drug resistance and stemness, have never been reported to be associated with the differential prognosis of Ewing sarcoma patients, we searched for novel IGF2BP3/mRNA interactions through *in silico* analysis using the catRAPID express web server tool (33). Among the 17 predicted genes with highest correlation parameters (correlation = 1, z-score $\geq$ 2), we chose *ABCF1*, a molecule described to be overexpressed in soft-tissue sarcomas (34), for further investigation. ABCF1 (also known as ABC50) is an ABC family member that does not possess membrane-spanning domains but associates with eukaryotic initiation factor 2 (eIF2) and ribosomes, likely functioning in mRNA translation (35–37). Beyond its biological significance, the role of ABCF1 in cancer has rarely been investigated. In Ewing sarcoma, the expression of ABCF1 was correlated with that of IGF2BP3 in patient-derived cell lines at both mRNA ($r = 0.75$, $P = 0.011$, Spearman test) and protein ($r = 0.83$, $P = 0.005$, Spearman test) levels (Fig. 3A; Supplementary Fig. S4A). The depletion of IGF2BP3 led to ABCF1 downregulation (Fig. 3B), while the transient overexpression of IGF2BP3 in LAP-35 cells, which display low levels of IGF2BP3, was correlated with increased ABCF1 levels (Fig. 3C). To investigate

Published OnlineFirst April 27, 2018; DOI: 10.1158/1078-0432.CCR-17-2602

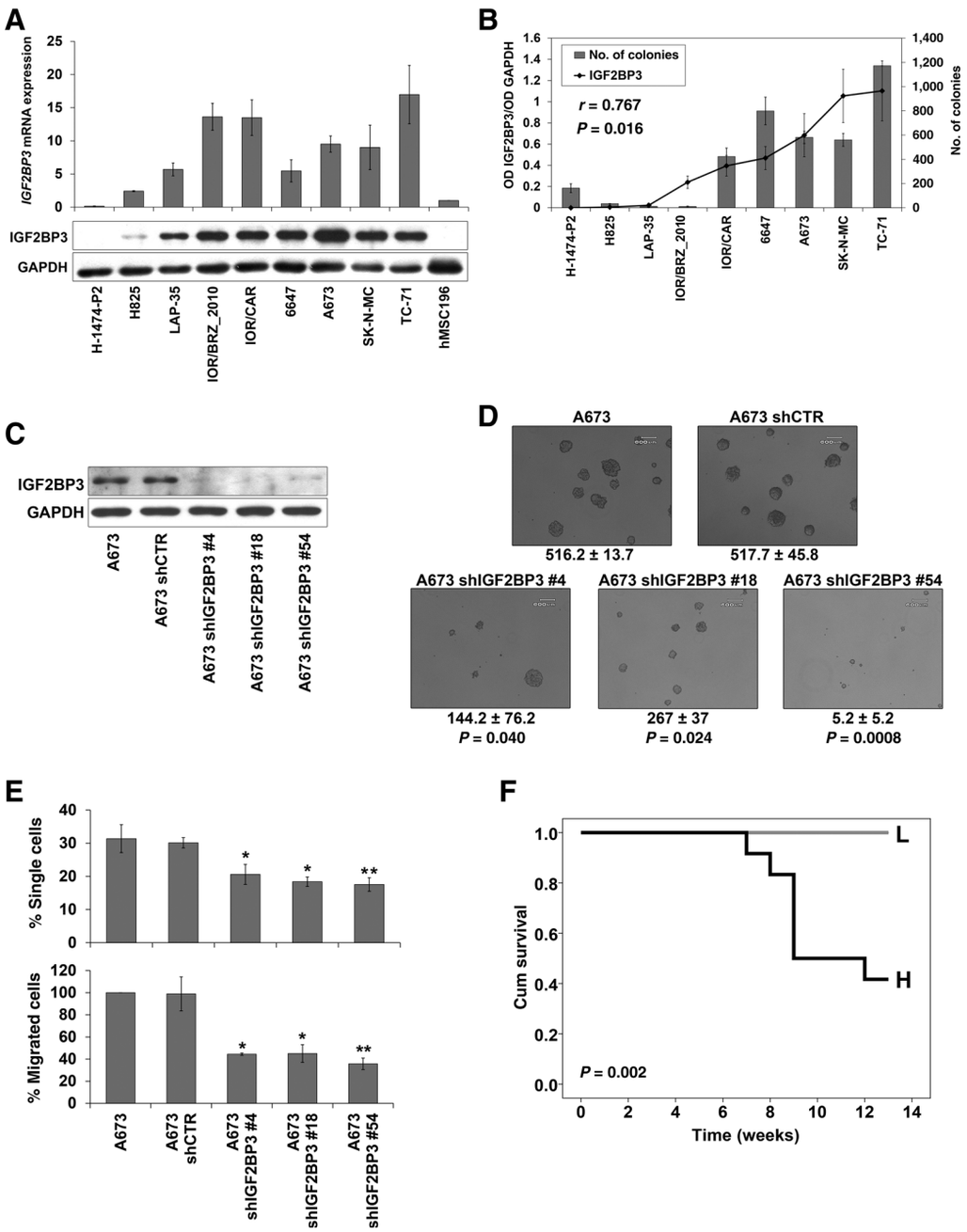

Figure 2.

Evaluation of the oncogenic potential of IGF2BP3 in Ewing sarcoma cell lines. **A,** Basal expression of IGF2BP3 in Ewing sarcoma cell lines. Top, relative mRNA expression levels of *IGF2BP3* compared with that of the calibrator (hMSC196; $2^{-\Delta\Delta C_t} = 1$). *GAPDH* was used as a housekeeping gene. Columns represent the mean values of three independent experiments, and the bars represent the SE. Bottom, Western blotting showing IGF2BP3 expression compared with that in hMSC196 cells. Equal sample loading was monitored by blotting for GAPDH. **B,** Protein expression of IGF2BP3 established by densitometry analysis (left *y*-axis) and clonogenic abilities of Ewing sarcoma cell lines (right *y*-axis). Points or columns represent the mean values of at least three independent experiments, and the bars represent the SE. **C,** Representative Western blotting showing IGF2BP3 expression in A673 cells depleted of IGF2BP3 compared with that in control (A673) or empty vector–transfected cells (A673 shCTR). GAPDH was used for normalization. **D,** Soft agar growth of IGF2BP3-silenced cells compared with that of controls. Mean ± SE of at least two independent experiments performed in duplicate and *P* values assessing statistical significance after one-way ANOVA with respect to A673 are shown below each image. **E,** Homotypic aggregation (top) and migration (bottom) of A673 cells depleted of IGF2BP3, control (A673), or empty vector–transfected cells (A673 shCTR). Columns represent the mean values of at least two independent experiments performed in triplicate, and the bars represent the SE. *, $P < 0.05$; **, $P < 0.01$, one-way ANOVA with respect to A673. **F,** Survival of Crl:CD-1-nu/nu Br mice after intravenous injection of A673 IGF2BP3-silenced cells compared with that of mice injected with control cells. Mice were grouped as "IGF2BP3 High" (black line; H) when A673 (6 mice) or A673 shCTR (6 mice) were injected, and "IGF2BP3 Low" (gray line; L) when A673 shIGF2BP3 #18 (6 mice) or A673 shIGF2BP3 #54 (6 mice) were injected (12 mice per group). Curve comparison was performed using log-rank test, and *P* values are shown. Time scale refers to weeks from injection.

Published OnlineFirst April 27, 2018; DOI: 10.1158/1078-0432.CCR-17-2602

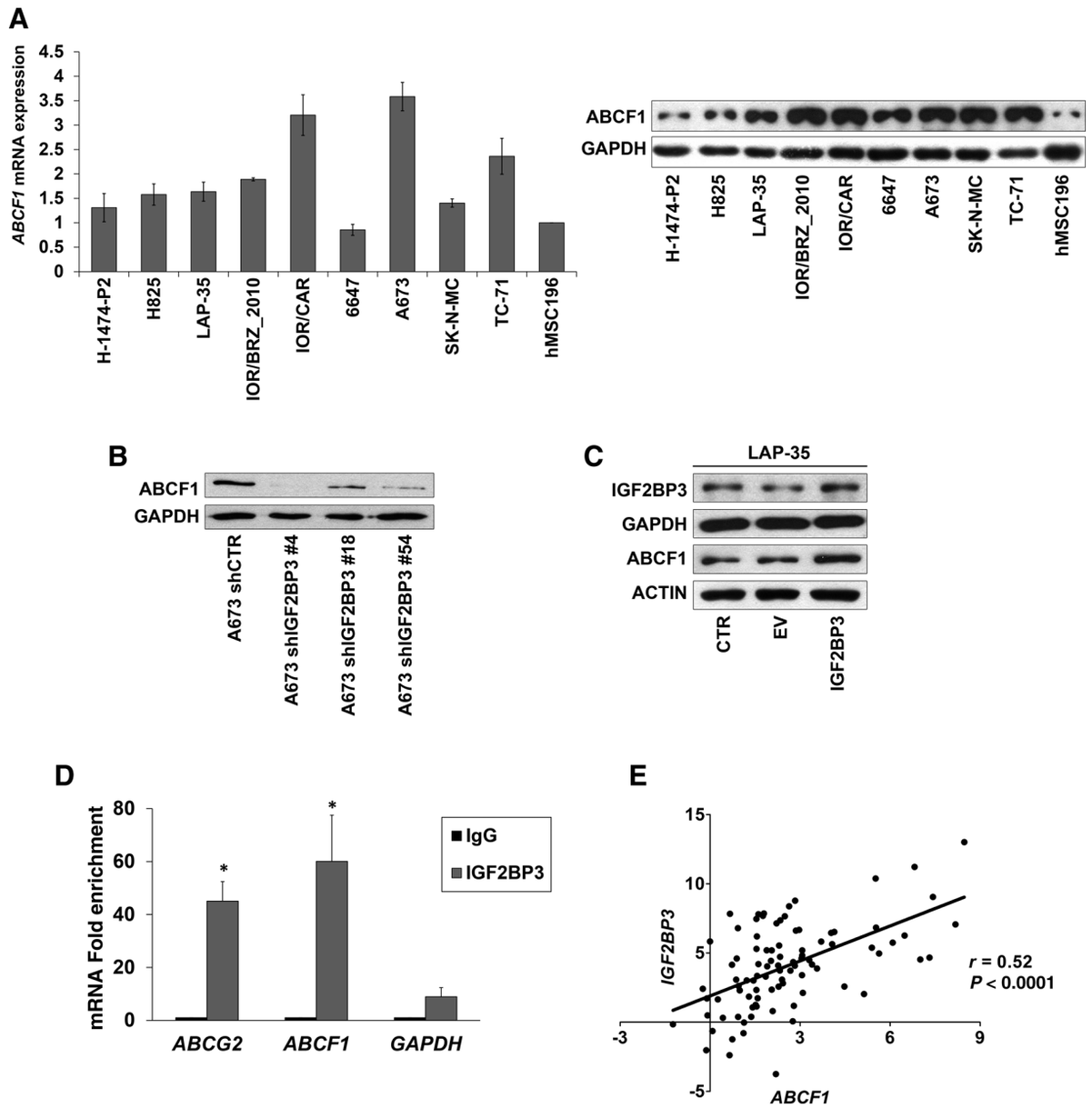

Figure 3.

Assessment of *ABCF1* as a novel IGF2BP3 mRNA target. **A,** Basal expression of ABCF1 in Ewing sarcoma cell lines. Left, relative mRNA expression levels of *ABCF1* compared with that of the calibrator (hMSC196; $2^{-\Delta\Delta C_t} = 1$). *GAPDH* was used as the housekeeping gene. Columns represent the mean values of two independent experiments, and the bars represent the SE. Right, Western blotting showing ABCF1 expression compared with that in hMSC196 cells. Equal sample loading was monitored by blotting for GAPDH. **B,** Western blotting showing ABCF1 expression in A673 cells depleted of IGF2BP3 compared with that in empty vector–transfected cells (A673 shCTR). GAPDH was used for normalization. **C,** Western blotting showing IGF2BP3 and ABCF1 levels after transient induction of IGF2BP3 expression. LAP-35 cells (CTR), transfected with empty vector (EV) or with plasmids encoding IGF2BP3 (IGF2BP3) were used. Cell lysates were collected after 24 hours of transfection. Equal loading was monitored using GAPDH. **D,** qRT-PCR analysis of IGF2BP3-associated mRNAs isolated from the cytoplasmic extracts of A673 cells by immunoprecipitation using an anti-IGF2BP3 antibody. Isotope control goat IgG was used as negative control. *ABCG2* and *GAPDH* were used as positive and negative controls, respectively. Columns represent the mean values of at least three independent experiments, and the bars represent the SE. *, $P < 0.05$, one-way ANOVA with respect to *GAPDH*. **E,** Scatter plot displaying the correlation between *IGF2BP3* and *ABCF1* mRNA expression in 99 Ewing sarcoma cases. Correlation coefficient (r) and P value were calculated using Pearson correlation analysis.

whether IGF2BP3 affects the steady-state levels of *ABCF1* mRNA, we used actinomycin D to inhibit transcription and measure the decay rate of *ABCF1*. Indeed, we observed a shorter *ABCF1* half-life in IGF2BP3-depleted cells than in control cells (Supplementary Fig. S4B). Direct protein–RNA interaction between IGF2BP3 and *ABCF1* was confirmed by ribo-immunoprecipitation (RIP) analysis. After immunoprecipitation (IP) with anti-IGF2BP3 antibody, the enrichment of selected transcripts was measured by

Published OnlineFirst April 27, 2018; DOI: 10.1158/1078-0432.CCR-17-2602

qRT-PCR, and we observed high enrichment of *ABCF*1 mRNA (Fig. 3D). As further evidence of the functional interaction between the two molecules, the expression of *ABCF1* in clinical samples (median = 2.27; range = 1.24–10.32; Supplementary Fig. S1D; Supplementary Table S4) was significantly correlated with that of *IGF2BP3* (Fig. 3E).

Although *ABCF1* did not predict Ewing sarcoma outcomes when considered as single biomarker (Supplementary Fig. S5A), the combined evaluation of *IGF2BP3* and *ABCF1* indicated a dichotomous behavior of *IGF2BP3* and *ABCF1* expression levels in the prediction of RFS (Supplementary Fig. S5B) and OS (Fig. 4A). Patients with high expression of *IGF2BP3* and low expression of *ABCF1* have poor prognoses (25% OS), while patients with low expression of *IGF2BP3* and high expression of *ABCF1* have good prognosis (85.5%). Multivariate analysis confirmed the statistical significance of the combined evaluation of *IGF2BP3* and *ABCF1* (Supplementary Table S6). When we considered individuals with the highest or lowest expression levels (75th percentile), the picture was even clearer. The 11 patients with the lowest expression of *IGF2BP3* and the highest expression of *ABCF1* did not experience any adverse events. In contrast, 9/14 patients with the highest expression of *IGF2BP3* and lowest expression of *ABCF1* experienced recurrence within 2 years (Supplementary Fig. S5C). Our hypothesis is that IGF2BP3 is the oncogenic driver, and *ABCF1* mRNA acts as a sponge that, by binding IGF2BP3, partly represses its functions. We chose two patient-derived cell lines (H825 and TC-71), representing the conditions of low *IGF2BP3* and high *ABCF1* expression (Fig. 4A, red line) or high *IGF2BP3* and high *ABCF1* expression (blue line in Fig. 4A), respectively, to verify the effect of *ABCF1* repression. When ABCF1 expression was silenced, the capability of Ewing sarcoma cells to form colonies was significantly increased (Fig. 4B), mimicking a tendency toward worse prognosis. qRT-PCR analysis after *ABCF1* silencing in TC-71 cells revealed that the mRNA levels of *ABCG2*, *MMP9*, and *CD44* were significantly increased, further indicating that lowering *ABCF1* levels freed up IGF2BP3 for binding to oncogenic mRNAs (Fig. 4C). To directly test the hypothesis that the interaction between *ABCF1* and IGF2BP3 can influence the ability of IGF2BP3 to bind target mRNAs, we silenced *ABCF1* in TC-71 cells and performed RIP assay to evaluate the interactions between IGF2BP3 and *ABCG2*, *MMP9* and *CD44* target mRNAs. As shown in Fig. 4D, the depletion of *ABCF1* enhanced the interaction of IGF2BP3 with its target mRNAs.

Patients with high *IGF2BP3* levels may benefit from treatment with the bromodomain and extraterminal domain (BET) inhibitor JQ1

Considering that the high expression of *IGF2BP3* negatively influences patient outcomes, we searched for treatments that can inhibit the expression of IGF2BP3. Limited knowledge is available regarding the molecular mechanisms responsible for IGF2BP3 regulation (38). However, the pharmacologic inhibition of IGF2BP3 expression via BET inhibition, both directly and indirectly, has been recently described in megakaryocytes and in B-ALL (19, 39). The treatment of three Ewing sarcoma cell lines, 6647, TC-71, and A673, representative of patients with poor prognosis (blue and light blue lines in survival curves, Fig. 4A), with the BETi JQ1 indeed resulted in a significant decrease in *IGF2BP3* expression and a parallel reduction in cellular growth under anchorage-independent conditions (Fig. 5A). The specificity of action of JQ1 on IGF2BP3 was further confirmed by the inhibitory effects on IGF2BP3 targets, such as ABCF1, *ABCG2*, *MMP9*, and *CD44* (Fig. 5B; Supplementary Fig. S6). In addition, A673 cells depleted of IGF2BP3 showed a lower sensitivity to JQ1 than cells transfected with empty vector control (Fig. 5C), further supporting a connection between JQ1 efficacy and IGF2BP3 expression. JQ1 has been shown to impair tumor growth in models relevant to childhood solid malignancies including Ewing sarcoma (40–42). However, the *in vivo* antitumor activity of JQ1 against solid tumors is relatively modest, with slowing of tumor growth without tumor regression and the need for other drugs to improve its therapeutic attractiveness (43). On the basis of recent evidence (44), we found that JQ1, in combination with the anti-microtubule drug VCR, an agent conventionally used in Ewing sarcoma systemic treatment, exerts additive effects on three Ewing sarcoma cell lines (Fig. 5D).

Discussion

In this study, we demonstrate for the first time that IGF2BP3 affects Ewing sarcoma aggressiveness and is a major determinant of Ewing sarcoma outcomes. The strong prognostic value of *IGF2BP3*, a novel therapeutic target, was validated in this study using explorative, training, and validation sets of patients with primary Ewing sarcoma using three different techniques. Because Ewing sarcoma is a rare tumor, it is difficult to organize large homogeneous cohorts of Ewing sarcoma patients without considering the heterogeneity of different chemotherapy regimens, surgical, and local treatments. We thus analyzed a relatively small but highly homogenous cohort of patients and corroborated clinical data with functional studies in patient-derived cell lines and/or IGF2BP3-silenced cells, *in vitro* and *in vivo*, to demonstrate that IGF2BP3 acts as a potent promoter of Ewing sarcoma malignancy. Several studies have described elevated expression of IGF2BP3 in human cancers, including osteosarcoma and leiomyosarcoma (38, 45), and provided evidence that IGF2BP3 plays essential roles in the modulation of tumor cell fate, stemness, migration, metastasis, and immune escape (46). Studies recently performed in immortalized hMSCs have demonstrated IGF2BPs within a dicer-resistant set of genes with a pan-cancer relevance in tumor development (47). In this study, we showed that IGF2BP3 increases the capacity of Ewing sarcoma cells to growth under anchorage-independent conditions, migrate and metastasize at distal organs, critical steps in targeted intervention, but does not affect the chemosensitivity of Ewing sarcoma cells to conventional chemotherapeutics. IGF2BP3 has been reported to confer resistance to platinum, doxorubicin, sorafenib, and mitoxantrone but not Taxol in ovarian cancer (17), breast cancer (48), and hepatocellular carcinoma (49), very likely through the modulation of hCTR1, a copper transporter involved in platinum uptake and ABCB1 and/or ABCG2, two members of the ABC superfamily transporters that are frequently involved in drug efflux. Discrepancies in these findings reflect the complex and cellular context–dependent interactions of IGF2BP3 with its targets. Indeed, despite the general consensus on the involvement of IGF2BP3 in tumorigenicity, the identification of downstream effectors of IGF2BP3, and mechanisms of action remain largely elusive. Recent iCLIP-Seq analysis showed that hundreds of mRNAs are bound by this protein (19, 50). In addition, IGF2BP3 modulates miRNA–mRNA interactions (50), further enhancing the level of

Published OnlineFirst April 27, 2018; DOI: 10.1158/1078-0432.CCR-17-2602

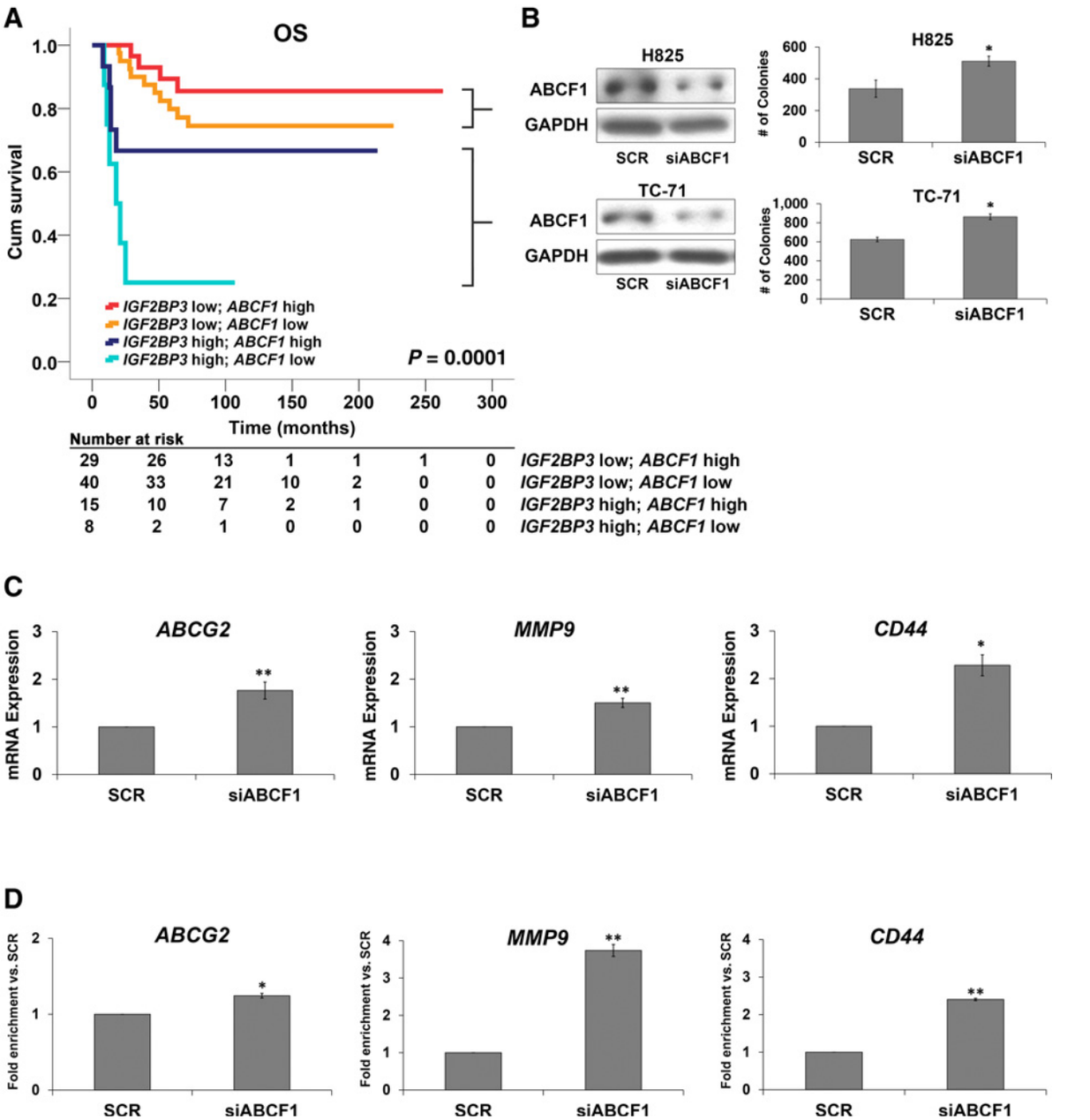

Figure 4.

Prognostic and functional impact of IGF2BP3/ABCF1 interaction in Ewing sarcoma. **A,** Prognostic value of *IGF2BP3* expression in combination with *ABCF1* expression according to Kaplan–Meier curves and log-rank test in the validation set of 99 Ewing sarcoma cases evaluated by qRT-PCR. High and low *IGF2BP3*-expressing samples were defined according to the 75th percentile values; high and low *ABCF1*-expressing samples were defined according to the median values. OS was considered. Time scale refers to months from diagnosis. Number of patients at risk are listed below each time interval. **B,** ABCF1 silencing was achieved in H825 (top) or TC-71 (bottom) cells after 96 or 48 hours of transfection, respectively, of siABCF1 (80 nmol/L) or scrambled control siRNA (SCR; 80 nmol/L). GAPDH was used as the loading control. Histograms represent soft-agar growth of H825 (top) or TC-71 (bottom) cells treated with siRNA or SCR. Mean ± SE of three independent experiments is shown (*, $P < 0.05$, Student *t* test). **C,** Impact of ABCF1 silencing on the expression of IGF2BP3 target mRNAs. *ABCG2, MMP9, and CD44* mRNA levels were measured by qRT-PCR in TC-71 cells after 72 hours of transfection of siABCF1 (80 nmol/L) or SCR (80 nmol/L). *GAPDH* was used as the housekeeping gene. Columns represent the mean values of at least two independent experiments, and the bars represent the SE (*, $P < 0.05$; **, $P < 0.01$, Student *t* test). **D,** qRT-PCR analysis of the relative binding of *ABCG2, MMP9*, and *CD44* mRNAs to IGF2BP3 isolated from the cytoplasmic extracts of TC-71 cells after 72 hours transfection of siABCF1 (80 nmol/L) or SCR (80 nmol/L). Histograms represent the fold enrichment over SCR for each siABCF1-treated sample. Isotope control goat IgG was used as negative control. Mean values and the SE of two independent experiments are shown. *, $P < 0.05$, Student *t* test.

Published OnlineFirst April 27, 2018; DOI: 10.1158/1078-0432.CCR-17-2602

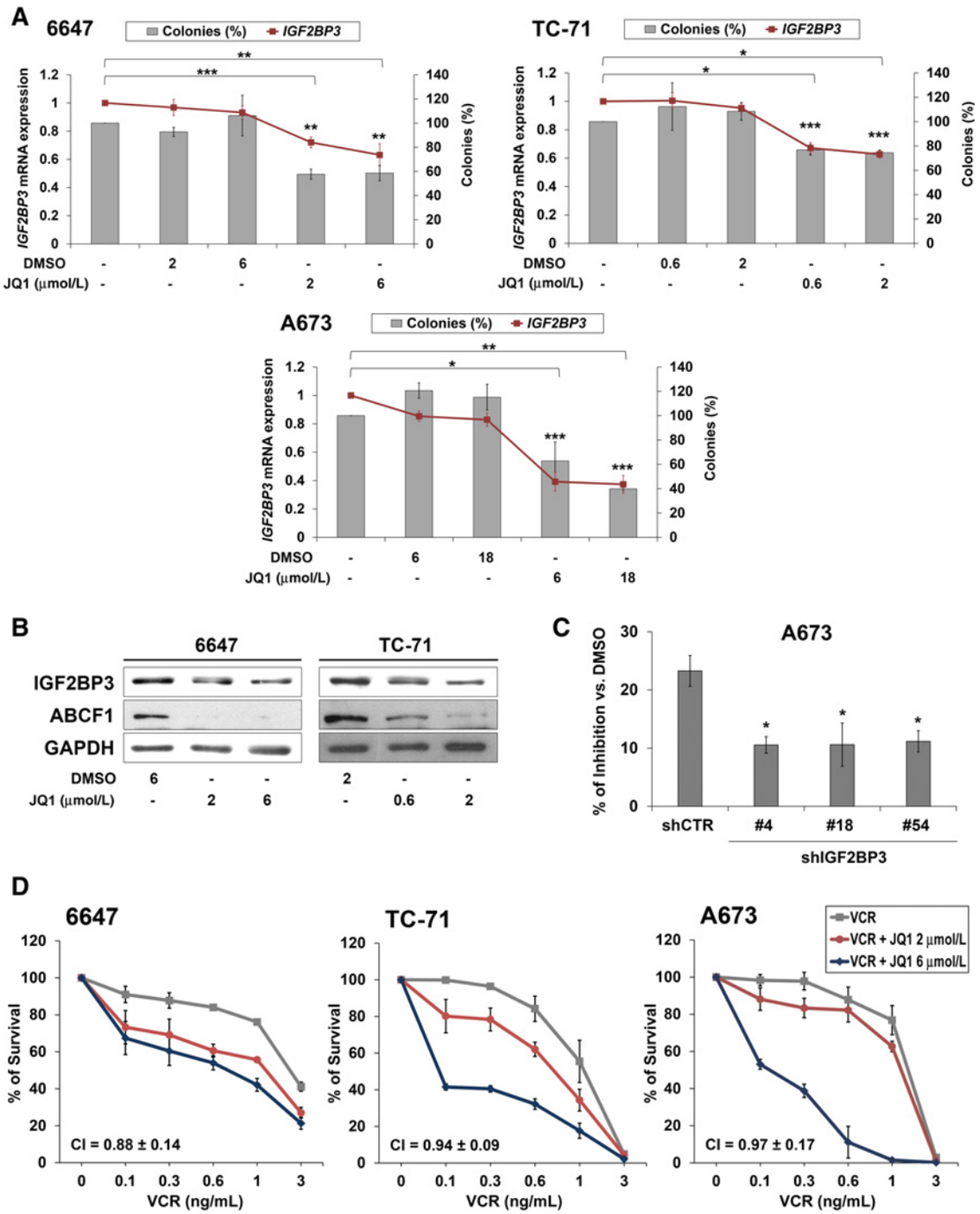

Figure 5.

Evaluation of benefits conferred by high IGF2BP3 expression in the response to BETi JQ1 alone or in combination with VCR in Ewing sarcoma cells. **A,** Relative *IGF2BP3* mRNA expression levels (left *y*-axis) and clonogenic abilities (right *y*-axis) of 6647, TC-71, and A673 cell lines after 48 hours of pretreatment with different doses of JQ1 or DMSO compared with that of untreated controls. Points or columns represent the mean values of at least three independent experiments, and the bars represent the SE (*, $P < 0.05$; **, $P < 0.01$; ***, $P < 0.001$, one-way ANOVA). **B,** Western blotting showing IGF2BP3 and ABCF1 expression in 6647 (left) or TC-71 (right) cells after 48-hour treatment with different doses of JQ1 or DMSO. GAPDH was used for normalization. **C,** Reversal of sensitivity to JQ1 in A673 cells depleted of IGF2BP3 compared with that in empty vector–transfected cells (A673 shCTR). Cells were treated for 48 hours with 1 μmol/L JQ1 or DMSO and percentage of inhibition as calculated by Trypan blue staining is shown. Columns represent the mean values of four independent experiments, and the bars represent the SE (*, $P < 0.05$, one-way ANOVA). **D,** Growth of 6647, TC-71, and A673 cells assessed using MTT assays after 72-hour exposure to VCR alone or in combination with JQ1. Results are displayed as the percentage of survival relative to that in controls. Doses and combination indexes (CI) are reported within each graph. Points, mean of three independent experiments; bars, SE.

Published OnlineFirst April 27, 2018; DOI: 10.1158/1078-0432.CCR-17-2602

complexity in the action of this RBP. Few mRNAs, including *IGF2*, *HMGA2*, *cyclin D1*, *MMP9*, *CD44*, and *ABCG2*, have been validated thus far as targets of IGF2BP3, and the interactions are strictly cellular context-specific (reviewed in refs. 15, 16). In this study, we identified *ABCF1* as a novel mRNA target of IGF2BP3 and provided evidence for new effects that severely affect Ewing sarcoma patient prognoses. High expression of ABCF1, a molecule involved in RNA translation (37, 51), but with still poorly understood functions, have been reported in soft-tissue sarcomas, including leiomyosarcoma, fibrosarcoma, and synovial sarcoma (34), and breast carcinoma (52). In these tumors and in Ewing sarcoma, as shown in this study, the levels of ABCF1, despite being higher than normal tissues or benign lesions, were not associated with differential patient prognoses. These data indicate that ABCF1 alone has a modest value as biomarker of tumor progression. However, we demonstrated here that *ABCF1* levels are correlated with those of *IGF2BP3* and that *ABCF1* mRNA alters the functions of IGF2BP3, serving as a sponge that limits the oncogenic potential of IGF2BP3. Moreover, IGF2BP3 binds to and stabilizes *ABCF1* mRNA. Silencing of ABCF1 increases the binding of IGF2BP3 to its target mRNAs, such as *CD44*, *MMP9*, and *ABCG2*, and enhances tumor aggressiveness. *ABCF1* depletion unlocks the oncogenic potential of IGF2BP3 and, therefore, patients with high expression of *IGF2BP3* and low, if any, expression of *ABCF1* are thought to experience rapid disease progression (with survival of 25% in patients with localized tumor). In contrast, when the levels of IGF2BP3 are low, the presence of *ABCF1* is sufficient to fully counteract its oncogenic functions and make patients prone to be cured. Thus, our data strongly support the simultaneous evaluation of *IGF2BP3* and *ABCF1* to stratify patients for differential treatments.

For cancer therapy, the presence of IGF2BP3 in cancer cells but not in healthy cells offers intriguing perspectives. The complexity of action of this oncogenic RBP, which exceeds that of classical oncogenes, supports the need of further research to elucidate additional target RNAs that IGF2BP3 can regulate to ultimately develop inhibitors that can prevent the effect of IGF2BP3 on tumor cells. Thus far, only an isocorydine derivative (d-ICD) or BETis have been demonstrated to hamper the expression of IGF2BP3 (19, 39, 49). Here, we provide evidence that the BETi JQ1, which has marked antitumor activity against several hematologic malignancies as well as solid tumors including Ewing sarcoma (41, 53, 54), decreases the expression of IGF2BP3 and some of its targets (ABCF1, *ABCG2*, *CD44*, *MMP9*) and suppressed the capacity of growth of Ewing sarcoma cells under anchorage-independent conditions. BET proteins are major epigenetic players, connecting chromatin structures with gene expression changes. BETis modulate tumor growth through direct and indirect mechanisms. In Ewing sarcoma, BETis repress EWS-FLI–driven gene signatures and downregulate important target genes in addition to affecting angiogenesis *in vivo* (40, 42). Here, we reported an additional effect leading to the impairment of Ewing sarcoma cell aggressiveness. The effect of JQ1 on IGF2BP3 expression is in fact EWS-FLI–independent, considering that this RBP is not regulated by the fusion product. The combination of JQ1 with VCR was shown to be additive, further supporting the use of BETis in the treatment of Ewing sarcoma patients with a high expression of IGF2BP3 and very low probabilities of survival. At least six clinical trials using BETis have been initiated in hematologic and solid tumors (NCT01713582, NCT02259114, NCT02296476, NCT01587703, NCT01987362, and NCT02158858), and manageable reversible toxicity has been observed (55, 56), indicating that the inclusion of these agents should be considered in the design of future clinical trials against Ewing sarcoma.

Disclosure of Potential Conflicts of Interest

No potential conflicts of interest were disclosed.

Authors' Contributions

Conception and design: C. Mancarella, P. Picci, K. Scotlandi
Development of methodology: C. Mancarella
Acquisition of data (provided animals, acquired and managed patients, provided facilities, etc.): M. Pasello, S. Ventura, L. Calzolari, L. Toracchio, P.L. Lollini, D.M. Donati, P. Picci, S. Ferrari
Analysis and interpretation of data (e.g., statistical analysis, biostatistics, computational analysis): C. Mancarella, M. Pasello, A. Grilli, P.L. Lollini, S. Ferrari, K. Scotlandi
Writing, review, and/or revision of the manuscript: C. Mancarella, K. Scotlandi
Study supervision: P. Picci, K. Scotlandi

Acknowledgments

This work was supported by the Italian Association for Cancer Research (IG2016_18451; to K. Scotlandi), and the Italian Ministry of Health (PROVABES project: PER-2011-2353839; to P. Picci and K. Scotlandi; RF Bando 2016; to K. Scotlandi). C. Mancarella was awarded the "Guglielmina Lucatello e Gino Mazzega" fellowship granted by Fondazione Italiana per la Ricerca sul Cancro-FIRC (FIRC project code: 17984) and partially supported by the Guido Berlucchi Foundation. The authors wish to thank Professor Guido Biasco, Dr. Annalisa Astolfi and Dr. Valentina Indio (Interdepartmental Center for Cancer Research "G. Prodi" (CIRC), University of Bologna, Bologna, Italy) for their support in RNA-seq and bioinformatics analyses. The authors are indebted to Professor Arthur M. Mercurio (Department of Molecular, Cell and Cancer Biology, University of Massachusetts Medical School, Worcester, MA, USA) for the plasmids for *IGF2BP3* silencing and overexpression. The authors also thank Cristina Ghinelli for editing the manuscript and Dr. Elettra Pignotti for revision of statistical analysis. The authors thank the Associazione "Un Sorriso con Luca" for encouraging our research.

The costs of publication of this article were defrayed in part by the payment of page charges. This article must therefore be hereby marked *advertisement* in accordance with 18 U.S.C. Section 1734 solely to indicate this fact.

Received September 7, 2017; revised February 12, 2018; accepted April 23, 2018; published first April 27, 2018.

References

1. Brohl AS, Solomon DA, Chang W, Wang J, Song Y, Sindiri S, et al. The genomic landscape of the Ewing Sarcoma family of tumors reveals recurrent STAG2 mutation. PLoS Genet 2014;10:e1004475.
2. Crompton BD, Stewart C, Taylor-Weiner A, Alexe G, Kurek KC, Calicchio ML, et al. The genomic landscape of pediatric Ewing sarcoma. Cancer Discov 2014;4:1326–41.
3. Tirode F, Surdez D, Ma X, Parker M, Le Deley MC, Bahrami A, et al. Genomic landscape of Ewing sarcoma defines an aggressive subtype with co-association of STAG2 and TP53 mutations. Cancer Discov 2014;4:1342–53.
4. Gaspar N, Hawkins DS, Dirksen U, Lewis IJ, Ferrari S, Le Deley MC, et al. Ewing sarcoma: current management and future approaches through collaboration. J Clin Oncol 2015;33:3036–46.

5. Paioli A, Luksch R, Fagioli F, Tamburini A, Cesari M, Palmerini E, et al. Chemotherapy-related toxicity in patients with non-metastatic Ewing sarcoma: influence of sex and age. J Chemother 2014;26:49–56.
6. Sheffield NC, Pierron G, Klughammer J, Datlinger P, Schonegger A, Schuster M, et al. DNA methylation heterogeneity defines a disease spectrum in Ewing sarcoma. Nat Med 2017;23:386–95.
7. Erkizan HV, Uversky VN, Toretsky JA. Oncogenic partnerships: EWS-FLI1 protein interactions initiate key pathways of Ewing's sarcoma. Clin Cancer Res 2010;16:4077–83.
8. Rocchi A, Manara MC, Sciandra M, Zambelli D, Nardi F, Nicoletti G, et al. CD99 inhibits neural differentiation of human Ewing sarcoma cells and thereby contributes to oncogenesis. J Clin Invest 2010;120:668–80.
9. Nakatani F, Ferracin M, Manara MC, Ventura S, Del Monaco V, Ferrari S, et al. miR-34a predicts survival of Ewing's sarcoma patients and directly influences cell chemo-sensitivity and malignancy. J Pathol 2012;226: 796–805.
10. Karnuth B, Dedy N, Spieker T, Lawlor ER, Gattenlohner S, Ranft A, et al. Differentially expressed miRNAs in Ewing sarcoma compared to mesenchymal stem cells: low miR-31 expression with effects on proliferation and invasion. PLoS One 2014;9:e93067.
11. Marques Howarth M, Simpson D, Ngok SP, Nieves B, Chen R, Siprashvili Z, et al. Long noncoding RNA EWSAT1-mediated gene repression facilitates Ewing sarcoma oncogenesis. J Clin Invest 2014;124:5275–90.
12. Marino MT, Grilli A, Baricordi C, Manara MC, Ventura S, Pinca RS, et al. Prognostic significance of miR-34a in Ewing sarcoma is associated with cyclin D1 and ki-67 expression. Ann Oncol 2014;25:2080–6.
13. Gerstberger S, Hafner M, Tuschl T. A census of human RNA-binding proteins. Nat Rev Genet 2014;15:829–45.
14. Scotlandi K, Remondini D, Castellani G, Manara MC, Nardi F, Cantiani L, et al. Overcoming resistance to conventional drugs in Ewing sarcoma and identification of molecular predictors of outcome. J Clin Oncol 2009; 27:2209–16.
15. Bell JL, Wachter K, Muhleck B, Pazaitis N, Kohn M, Lederer M, et al. Insulin-like growth factor 2 mRNA-binding proteins (IGF2BPs): post-transcriptional drivers of cancer progression? Cell Mol Life Sci 2013; 70:2657–75.
16. Lederer M, Bley N, Schleifer C, Huttelmaier S. The role of the oncofetal IGF2 mRNA-binding protein 3 (IGF2BP3) in cancer. Semin Cancer Biol 2014; 29:3–12.
17. Hsu KF, Shen MR, Huang YF, Cheng YM, Lin SH, Chow NH, et al. Overexpression of the RNA-binding proteins Lin28B and IGF2BP3 (IMP3) is associated with chemoresistance and poor disease outcome in ovarian cancer. Br J Cancer 2015;113:414–24.
18. Lochhead P, Imamura Y, Morikawa T, Kuchiba A, Yamauchi M, Liao X, et al. Insulin-like growth factor 2 messenger RNA binding protein 3 (IGF2BP3) is a marker of unfavourable prognosis in colorectal cancer. Eur J Cancer 2012;48:3405–13.
19. Palanichamy JK, Tran TM, Howard JM, Contreras JR, Fernando TR, Sterne-Weiler T, et al. RNA-binding protein IGF2BP3 targeting of oncogenic transcripts promotes hematopoietic progenitor proliferation. J Clin Invest 2016;126:1495–511.
20. Bacci G, Longhi A, Ferrari S, Mercuri M, Versari M, Bertoni F. Prognostic factors in non-metastatic Ewing's sarcoma tumor of bone: an analysis of 579 patients treated at a single institution with adjuvant or neoadjuvant chemotherapy between 1972 and 1998. Acta Oncol 2006;45:469–75.
21. Ferrari S, Sundby Hall K, Luksch R, Tienghi A, Wiebe T, Fagioli F, et al. Nonmetastatic Ewing family tumors: high-dose chemotherapy with stem cell rescue in poor responder patients. Results of the Italian Sarcoma Group/Scandinavian Sarcoma Group III protocol. Ann Oncol 2011;22: 1221–7.
22. Khoury JD.Ewing sarcoma family of tumors: a model for the new era of integrated laboratory diagnostics. Expert Rev Mol Diagn 2008;8: 97–105.
23. Toomey EC, Schiffman JD, Lessnick SL. Recent advances in the molecular pathogenesis of Ewing's sarcoma. Oncogene 2010;29:4504–16.
24. Picci P, Bohling T, Bacci G, Ferrari S, Sangiorgi L, Mercuri M, et al. Chemotherapy-induced tumor necrosis as a prognostic factor in localized Ewing's sarcoma of the extremities. J Clin Oncol 1997;15:1553–9.
25. Dupont WD, Plummer WD Jr.Power and sample size calculations for studies involving linear regression. Control Clin Trials 1998;19:589–601.
26. Kim D, Pertea G, Trapnell C, Pimentel H, Kelley R, Salzberg SL. TopHat2: accurate alignment of transcriptomes in the presence of insertions, deletions and gene fusions. Genome biology 2013;14:R36.
27. Anders S, Pyl PT, Huber W. HTSeq–a Python framework to work with high-throughput sequencing data. Bioinformatics 2015;31:166–9.
28. Robinson MD, Oshlack A. A scaling normalization method for differential expression analysis of RNA-seq data. Genome Biol 2010;11:R25.
29. Bradburn MJ, Clark TG, Love SB, Altman DG. Survival analysis Part III: multivariate data analysis – choosing a model and assessing its adequacy and fit. Br J Cancer 2003;89:605–11.
30. Chou TC, Motzer RJ, Tong Y, Bosl GJ. Computerized quantitation of synergism and antagonism of taxol, topotecan, and cisplatin against human teratocarcinoma cell growth: a rational approach to clinical protocol design. J Natl Cancer Inst 1994;86:1517–24.
31. Huang HY, Illei PB, Zhao Z, Mazumdar M, Huvos AG, Healey JH, et al. Ewing sarcomas with p53 mutation or p16/p14ARF homozygous deletion: a highly lethal subset associated with poor chemoresponse. J Clin Oncol 2005;23:548–58.
32. Horibata S, Vo TV, Subramanian V, Thompson PR, Coonrod SA. Utilization of the soft agar colony formation assay to identify inhibitors of tumorigenicity in breast cancer cells. J Vis Exp 2015;99:52727.
33. Agostini F, Zanzoni A, Klus P, Marchese D, Cirillo D, Tartaglia GG. catRAPID omics: a web server for large-scale prediction of protein-RNA interactions. Bioinformatics 2013;29:2928–30.
34. Cunha IW, Carvalho KC, Martins WK, Marques SM, Muto NH, Falzoni R, et al. Identification of genes associated with local aggressiveness and metastatic behavior in soft tissue tumors. Transl Oncol 2010; 3:23–32.
35. Tyzack JK, Wang X, Belsham GJ, Proud CG. ABC50 interacts with eukaryotic initiation factor 2 and associates with the ribosome in an ATP-dependent manner. J Biol Chem 2000;275:34131–9.
36. Paytubi S, Morrice NA, Boudeau J, Proud CG. The N-terminal region of ABC50 interacts with eukaryotic initiation factor eIF2 and is a target for regulatory phosphorylation by CK2. Biochem J 2008;409:223–31.
37. Paytubi S, Wang X, Lam YW, Izquierdo L, Hunter MJ, Jan E, et al. ABC50 promotes translation initiation in mammalian cells. J Biol Chem 2009; 284:24061–73.
38. Ueki A, Shimizu T, Masuda K, Yamaguchi SI, Ishikawa T, Sugihara E, et al. Up-regulation of Imp3 confers in vivo tumorigenicity on murine osteosarcoma cells. PLoS One 2012;7:e50621.
39. Elagib KE, Lu CH, Mosoyan G, Khalil S, Zasadzinska E, Foltz DR, et al. Neonatal expression of RNA-binding protein IGF2BP3 regulates the human fetal-adult megakaryocyte transition. J Clin Invest 2017;127: 2365–77.
40. Bid HK, Phelps DA, Xaio L, Guttridge DC, Lin J, London C, et al. The bromodomain BET Inhibitor JQ1 suppresses tumor angiogenesis in models of childhood sarcoma. Mol Cancer Ther 2016;15:1018–28.
41. Jacques C, Lamoureux F, Baud'huin M, Rodriguez Calleja L, Quillard T, Amiaud J, et al. Targeting the epigenetic readers in Ewing sarcoma inhibits the oncogenic transcription factor EWS/Fli1. Oncotarget 2016; 7:24125–40.
42. Loganathan SN, Tang N, Fleming JT, Ma Y, Guo Y, Borinstein SC, et al. BET bromodomain inhibitors suppress EWS-FLI1-dependent transcription and the IGF1 autocrine mechanism in Ewing sarcoma. Oncotarget 2016; 7:43504–17.
43. Ott CJ, Kopp N, Bird L, Paranal RM, Qi J, Bowman T, et al. BET bromodomain inhibition targets both c-Myc and IL7R in high-risk acute lymphoblastic leukemia. Blood 2012;120:2843–52.
44. Liu PY, Sokolowski N, Guo ST, Siddiqi F, Atmadibrata B, Telfer TJ, et al. The BET bromodomain inhibitor exerts the most potent synergistic anticancer effects with quinone-containing compounds and anti-microtubule drugs. Oncotarget 2016;7:79217–32.
45. Cornejo K, Shi M, Jiang Z. Oncofetal protein IMP3: a useful diagnostic biomarker for leiomyosarcoma. Hum Pathol 2012;43:1567–72.
46. Schmiedel D, Tai J, Yamin R, Berhani O, Bauman Y, Mandelboim O. The RNA binding protein IMP3 facilitates tumor immune escape by down-regulating the stress-induced ligands ULPB2 and MICB. Elife 2016;5: pii: e13426.
47. JnBaptiste CK, Gurtan AM, Thai KK, Lu V, Bhutkar A, Su MJ, et al. Dicer loss and recovery induce an oncogenic switch driven by

Published OnlineFirst April 27, 2018; DOI: 10.1158/1078-0432.CCR-17-2602

transcriptional activation of the oncofetal Imp1-3 family. Genes Dev 2017;31:674–87.
48. Samanta S, Pursell B, Mercurio AM. IMP3 protein promotes chemoresistance in breast cancer cells by regulating breast cancer resistance protein (ABCG2) expression. J Biol Chem 2013;288:12569–73.
49. Li M, Zhang L, Ge C, Chen L, Fang T, Li H, et al. An isocorydine derivative (d-ICD) inhibits drug resistance by downregulating IGF2BP3 expression in hepatocellular carcinoma. Oncotarget 2015;6:25149–60.
50. Ennajdaoui H, Howard JM, Sterne-Weiler T, Jahanbani F, Coyne DJ, Uren PJ, et al. IGF2BP3 modulates the interaction of invasion-associated transcripts with RISC. Cell Rep 2016;15:1876–83.
51. Stewart JD, Cowan JL, Perry LS, Coldwell MJ, Proud CG. ABC50 mutants modify translation start codon selection. Biochem J 2015;467:217–29.
52. Hlavac V, Brynychova V, Vaclavikova R, Ehrlichova M, Vrana D, Pecha V, et al. The expression profile of ATP-binding cassette transporter genes in breast carcinoma. Pharmacogenomics 2013;14:515–29.
53. Boi M, Todaro M, Vurchio V, Yang SN, Moon J, Kwee I, et al. Therapeutic efficacy of the bromodomain inhibitor OTX015/MK-8628 in ALK-positive anaplastic large cell lymphoma: an alternative modality to overcome resistant phenotypes. Oncotarget 2016;7:79637–53.
54. Stathis A, Zucca E, Bekradda M, Gomez-Roca C, Delord JP, de La Motte Rouge T, et al. Clinical response of carcinomas harboring the BRD4-NUT oncoprotein to the targeted bromodomain inhibitor OTX015/MK-8628. Cancer Discov 2016;6:492–500.
55. Amorim S, Stathis A, Gleeson M, Iyengar S, Magarotto V, Leleu X, et al. Bromodomain inhibitor OTX015 in patients with lymphoma or multiple myeloma: a dose-escalation, open-label, pharmacokinetic, phase 1 study. Lancet Haematol 2016;3:e196–204.
56. Berthon C, Raffoux E, Thomas X, Vey N, Gomez-Roca C, Yee K, et al. Bromodomain inhibitor OTX015 in patients with acute leukaemia: a dose-escalation, phase 1 study. Lancet Haematol 2016; 3:e186–95.

Published OnlineFirst April 27, 2018; DOI: 10.1158/1078-0432.CCR-17-2602

Clinical Cancer Research

Insulin-Like Growth Factor 2 mRNA-Binding Protein 3 is a Novel Post-Transcriptional Regulator of Ewing Sarcoma Malignancy

Caterina Mancarella, Michela Pasello, Selena Ventura, et al.

Clin Cancer Res 2018;24:3704-3716. Published OnlineFirst April 27, 2018.